JOC The Journal of Organic Chemistry

Article

pubs.acs.org/joc

"Ene" Reactions of Singlet Oxygen at the Air–Water Interface

Belaid Malek,[†] William Fang,[†] Inna Abramova,[†] Niluksha Walalawela,[†,‡] Ashwini A. Ghogare,[†,‡] and Alexander Greer*[,†,‡]

[†]Department of Chemistry, Brooklyn College of the City University of New York, Brooklyn, New York 11210, United States

[‡]Ph.D. Program in Chemistry, The Graduate Center of the City University of New York, 365 Fifth Avenue, New York, New York 10016, United States

Supporting Information

ABSTRACT: Prenylsurfactants [$(CH_3)_2C{=}CH(CH_2)_nSO_3^-$ Na^+ (n = 4, 6, or 8)] were designed to probe the "ene" reaction mechanism of singlet oxygen at the air–water interface. Increasing the number of carbon atoms in the hydrophobic chain caused an increase in the regioselectivity for a secondary rather than tertiary surfactant hydroperoxide, arguing for an orthogonal alkene on water. The use of water, deuterium oxide, and H_2O/D_2O mixtures helped to distinguish mechanistic alternatives to homogeneous solution conditions that include dewetting of the π bond and an unsymmetrical perepoxide transition state in the hydroperoxide-forming step. The prenylsurfactants and a photoreactor technique allowed a certain degree of interfacial control of the hydroperoxidation reaction on a liquid support, where the oxidant (airborne $^1O_2$) is delivered as a gas.

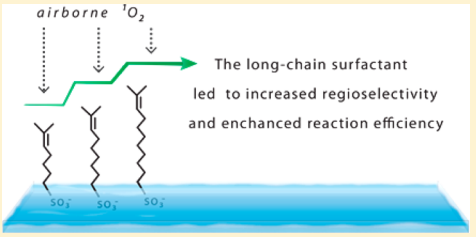

INTRODUCTION

The properties of reactive oxygen species (ROS) at interfaces in organic chemistry are of interest,[1−6] but answers to basic questions are needed. How can ROS such as $^1O_2$ be probed at interfaces? One way is to use trapping agents that reside at the interface, which is the topic of this paper. We report the use of prenylsurfactants **1**–**3** in probing $^1O_2$ at the air–water interface (Figure 1) and find that an increase in chain length minimizes contact of the alkene group with water unlike $^1O_2$ reactions in the bulk solution phase.

Previous papers have reported the properties of ROS at interfaces, such as aerosol and organic film oxidation by beams of hydroxyl radicals using reflection/absorption IR spectroscopy.[7] (Air–water interface reactions are often monitored by viscosity or surface potential, area, and pressure.[8]) Micellar studies have analyzed the kinetics of $^1O_2$ in the two phases[9,10] but did not consider the residence of $^1O_2$ at the interface. Flow reactors for $^1O_2$ generation in water are coming into use[11−18] and can be applied to interfacial $^1O_2$ studies.[19−22] Also, compound hydrophobicity has been exploited for selectivity in "on water" organic reactions,[23−28] but further insight into the interaction of $^1O_2$ at air–water interfaces is needed.

Here, surfactants **1**–**3** are used for an interfacial $^1O_2$ reaction. A feature of **1**–**3** is the prenyl (2-methyl-2-butene) group, which has been shown to react with $^1O_2$ in organic compounds.[29−36] Our prenylsurfactants were designed so that the sulfonate anion is solvated and removed from the 2-methyl-2-butene group, revealing air–water interface effects. Our hypothesis was that prenylsurfactants that vary in chain length can be adjusted to probe interfacial $^1O_2$ reactivity where long-chain prenyls would extend into the gap between the liquid surface and the solid sensitizer. Our previous work showed that **2** reacted with airborne $^1O_2$,[37,38] but no information about a possible chain-length dependence was available.

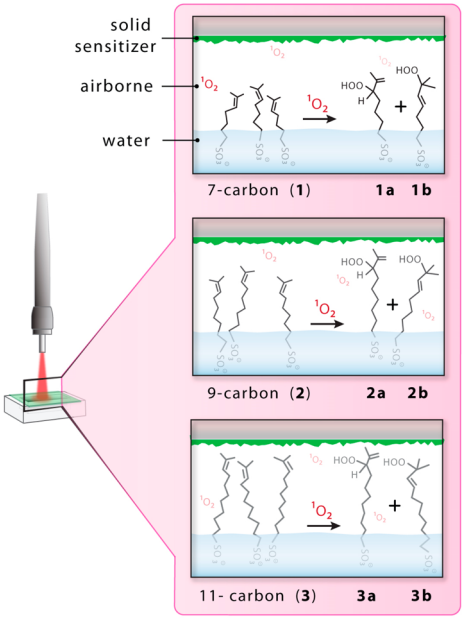

Figure 1. Reactor for the delivery of airborne $^1O_2$ to **1**–**3** at the air–water interface. Red light is directed via an optical fiber to a silica plate coated with a phthalocyanine sensitizer that sits above the water solution. The reaction of $^1O_2$ with the prenyl groups led to the formation of secondary (**a**) and tertiary (**b**) hydroperoxides.

Received: May 3, 2016
Published: July 6, 2016

DOI: 10.1021/acs.joc.6b01030
J. Org. Chem. 2016, 81, 6395−6401

Here, we report on the screening of surfactants **1**−**3** in an attempt to probe the role of chain length in interfacial $^1O_2$ reactions. In particular, we (1) synthesized prenylsurfactants **1**−**3** using an oxidation/Wittig/Strecker reaction sequence and computed their solubility, (2) quantitated their reactivity with $^1O_2$ as the percent yield, (3) determined the regioselective preference for secondary over tertiary hydroperoxides, and (4) utilized homogeneous conditions as a means to turn off the regioselectivity.

RESULTS AND DISCUSSION

Synthesis and Solubility. The synthesis of prenylsurfactants **1**−**3** was performed in three steps (Scheme 1). First, the reaction of bromo-alkanols **4** and **5** with PCC was required, which led to aldehydes **6** and **7**, respectively. Second, a Wittig reaction was conducted on **6** or **7** with isopropylphosphonium iodide, followed by a reaction with *n*-butyllithium leading to mixtures of bromo- and iodoalkenes **8**−**11**. Third, a Strecker reaction was performed using either 9-bromo-2-methylnon-2-ene or mixtures of **8** and **9** or **10** and **11** with sodium sulfite in a refluxing DMF/water solution (1:1). Surfactant **2** was known from previous work.[37] After workup, off-white solid products of **1**−**3** were obtained, which bore marginal water solubility. Computed solubilities of **1**−**3** were calculated using the ACD algorithm.[39] The computed partition coefficients (log *P*) in Table 1 show an ∼2 log increase as the surfactant chain length increased from 7 to 11 carbons. Literature reports on other olefin sulfonates have shown that as chain length decreases the water solubility increases.[40] Next, we placed surfactants **1**−**3** into a singlet oxygen reactor and sought reactivity patterns based on chain length.

Scheme 1. Synthesis of Heptene, Nonene, and Undecene Sulfonates 1−3

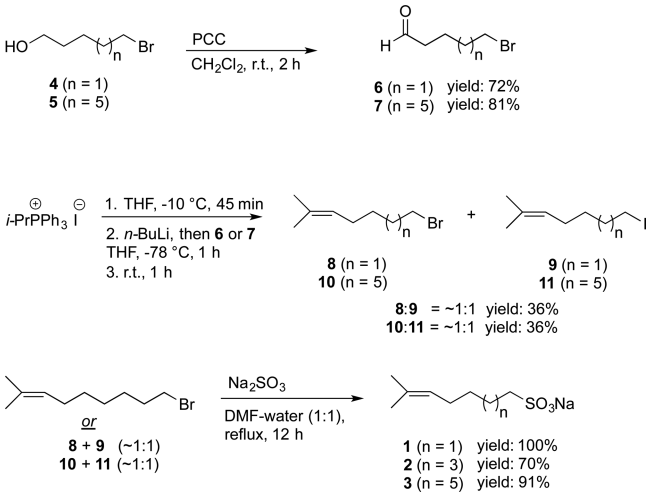

Singlet Oxygen Reactor. Our reactor uses liquid samples of **1**, **2**, or **3** irradiated from above with red light to a silica plate coated with aluminum(III) phthalocyanine chloride tetrasulfonic acid (AlPcS) (Figure 2). AlPcS[41−46] produces $^1O_2$ where our reactor is unique in that the plate coated with the phthalocyanine is placed above the solution and is physically separated from the water phase. There are air-gap distances of 0.4 and 1.5 mm from the sensitizer plate to the water surface at the walls of the cuvette and the middle of the meniscus, respectively. When we conduct a $^1O_2$ lifetime (τ_Δ) measurement by NIR luminescence, a 0.5 ms lifetime for airborne $^1O_2$ is found in the air gap above the air−liquid interface (Figure S24). We also investigated the air-gap distance to see whether the $^1O_2$

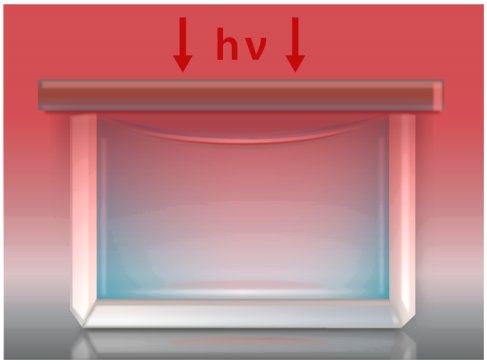

Figure 2. Singlet oxygen reactor in which airborne $^1O_2$ forms by red-light irradiation of a silica plate with aluminum(III) phthalocyanine chloride tetrasulfonic acid deposited on its bottom side. Singlet oxygen migrates through air to surfactants **1**−**3** at the liquid surface underneath. The surfactant traps airborne $^1O_2$ at the air−water interface, a location that contains no sensitizer.

Table 1. Effects of Increasing the Chain Length of the Surfactant on the Computed Solubility, Percent Yield, and Ratio of Hydroperoxides Formed by Ene $^1O_2$ Reactions[a]

			surfactant[b]		singlet oxygen			
entry	compound	computed log *P*[a]	chain length	solvation state	interfacial	solvent	% yield (**a** + **b**)[c,d]	**a**:**b** product ratio
1	**1**	1.40 ± 0.43	7	not solvated	air−liquid	D_2O	76 ± 3	2.5:1
2	**2**	2.39 ± 0.43	9	not solvated	air−liquid	D_2O	82 ± 2	2.8:1
3	**2**		9	not solvated	air−liquid	D_2O/H_2O (3:1, v:v)	64	2.8:1
4	**2**		9	not solvated	air−liquid	D_2O/H_2O (1:1, v:v)	58	2.8:1
5	**2**		9	not solvated	air−liquid	D_2O/H_2O (1:3, v:v)	39	2.8:1
6	**2**		9	not solvated	air−liquid	H_2O	∼25 ± 10	2.8:1
7	**3**	3.46 ± 0.43	11	not solvated	air−liquid	D_2O	85 ± 2	3.2:1
8	**2**[e]		9	solvated	air−liquid	CH_3CN/H_2O (9:1)	46 ± 5	1.3:1
9	**2**[e]		9	solvated	air−liquid	CD_3CN/D_2O (9:1)	100 ± 1	1:1
10	2-methyl-2-pentene[f]		–	solvated	–	CH_3CN	–	1.4:1

[a]Log *P* values were computed with an ACD program. [b]Samples of 1 mM surfactant in 0.6 mL were irradiated by a 669 nm laser via an optical fiber above the sensitizer solid for 1 h. [c]Trace products such as ketones or epoxides from alternative mechanisms (i.e., non-$^1O_2$ reactions) were not observed. [d]Errors are expressed as means ± the standard deviation. [e]From ref 38. [f]From ref 36.

DOI: 10.1021/acs.joc.6b01030
J. Org. Chem. 2016, 81, 6395−6401

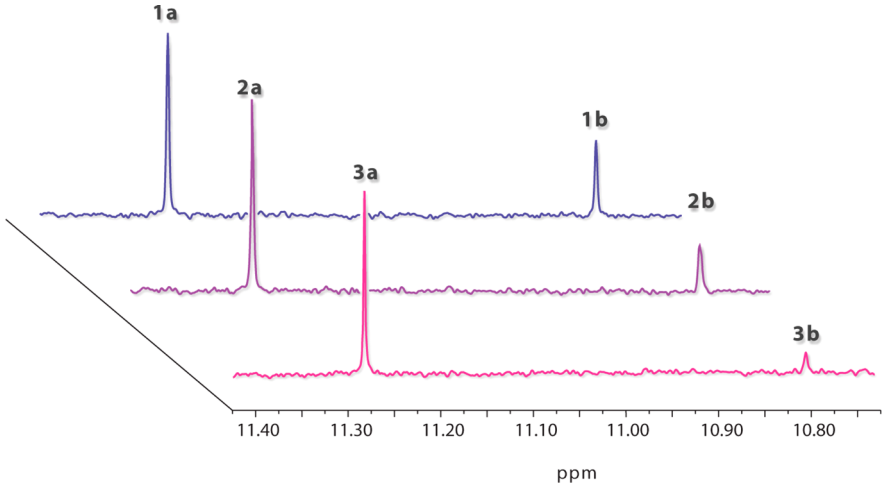

Figure 3. ^{1}H NMR spectra of secondary (**a**) and tertiary (**b**) hydroperoxides from the reaction of $^1O_2$ with **1**−**3** at the air−water interface.

distance traveled would relate to product yield, which it does. When the sensitizer plate-to-water distance was increased from 0.4 to 0.9 mm and then to 1.4 mm measured at the cuvette walls, airborne singlet oxygenation of **2** showed 82, 17, and 0% hydroperoxide yields, respectively (Figure S15), demonstrating the requirement for $^1O_2$. The next step was to examine the hydroperoxidation efficiency in surfactants **1**−**3**.

Table 1 shows the amount of hydroperoxides formed on the basis of chain length. The yield of hydroperoxides was found to be greater in **3** (85%, entry 7) than in **2** (82%, entry 2) and **1** (76%, entry 1) after 1 h. The increase is nearly linearly related to the length of the prenylsurfactant. Other conditions, namely using deuterated solvents to increase the $^1O_2$ lifetime, were then investigated. The hydroperoxide yields for the reaction of **2** with $^1O_2$ at the air−water interface increased by ∼3-fold in D_2O compared to that in H_2O (the yield of **2a** and **2b** was 82% in D_2O and ∼25% in H_2O) (Table 1, entries 2 and 6), and there were increases in yield when the D_2O:H_2O ratio changed from 1:3 to 3:1 (entries 3−5). Given enough time, the use of D_2O or H_2O will reach the same final yields, even though deuterated solvents reach higher $^1O_2$ product yields more rapidly than protio solvents do. That is, a 20-fold enhanced product yield would have been expected if the hydroperoxidation of **2** occurred in the bulk solution phase, where the $^1O_2$ lifetime is longer in D_2O (τ_Δ = 69 μs) than in H_2O (τ_Δ = 3.5 μs).[47−49] Thus, the results are consistent with partial solvation of **2** and point to a dependence of chain length on regioselectivity, as will be seen next.

Regioselective Ene $^1O_2$ Reactions. Table 1 shows the relative amount of hydroperoxides **a** and **b** formed from the reaction of airborne $^1O_2$ with **1**−**3**. Note the regioselective preference for hydroperoxide **a** over **b** increased from a ratio of 2.5:1 to 3.2:1 for **1** compared to **3** at the air−water interface (Table 1, entries 1, 2, and 7). ^{1}H NMR spectra show larger amounts of the secondary hydroperoxide formed as the surfactant chain length increased (Figure 3). However, the regioselectivity is lost for the reaction of airborne $^1O_2$ with solvated surfactant **2** in aqueous acetonitrile (Table 1, entries 8 and 9), which is similar to the lack of regioselectivity in the homogeneous singlet oxygen reaction with 2-methyl-2-pentene[36] in acetonitrile (Table 1, entry 10). The data reported in Table 1 (entries 1−9) were recorded with a concentration of 1 mM for surfactants **1**−**3** to examine the yield and regioselectivity, where the reactions were performed to high percent conversion of hydroperoxides **a** and **b**, because we previously found micelle formation for **2** above 10 mM and the loss of regioselectivity at 25 mM.[38] Previous work[38] also indicated the importance of added Ca^{2+} ions in prenylsurfactant **2** photoperoxidation where salting out led to an increase in its suspending power and a loss of regioselectivity. The regioselectivity can also be reversed; there have been reports of trisubstituted alkenes with bulky allylic substituents that form tertiary over secondary hydroperoxides,[50,51] which is a reversal of the regioselectivity that we observe with formation of secondary over tertiary hydroperoxides in **1**−**3**.

Our observed regioselectivity was not due to hydroperoxide instability. We examined hydroperoxides **a** and **b** and found them to be reasonably stable; for example, complete decomposition of **2a** required 1 h at 100 °C, and that of **2b** required 2 h at 185 °C, where the decomposition products were not scrutinized. Thus, alternative mechanisms such as the Schenck rearrangement (radical $^{\bullet}$OOH migration) that would afford alternative hydroperoxides can be ruled out.[52−54] As will be seen in the next section, the regioselectivity of hydroperoxide **a** over **b** is attributed to the prenyl groups of **1**−**3** extended away from the water surface.

Mechanistic Aspects. Our chain-length study has permitted quantitative measurements of "ene" reactions of $^1O_2$ at the air−water interface. Two types of correlations were found as the chain length increased in surfactants **1**−**3**. First, the hydroperoxide percent yield increased nearly linearly from 76 to 85%, in which spatial separation is likely important on the basis of the number of -CH_2- groups, where the distances between the surfactant head and the methyl termini range from 10.9 to 16.0 Å (Figure 4). Second, the regioselectivity also correlated linearly; Figure 4 (red line) shows the plot of the data from entries 1, 2, and 4 in Table 1, in which each additional -CH_2- group in the chain accounted for an ∼3% increase in **a** over **b**. Further support for an interfacial mechanism is the loss of regioselectivity when **1**−**3** were dissolved in a homogeneous solution, similar to that seen for 2-methyl-2-pentene dissolved in organic solvents.[36]

Mechanistically, the longer chain minimizes contact between the prenyl group and water, for preferential allylic hydrogen abstraction of the methyl groups by airborne $^1O_2$. The methylene allylic hydrogens are less accessible, making the methyl hydrogen abstraction favorable. This interpretation, along with the D_2O result (Table 1, entries 2 and 6) of a sparse

DOI: 10.1021/acs.joc.6b01030
J. Org. Chem. 2016, 81, 6395−6401

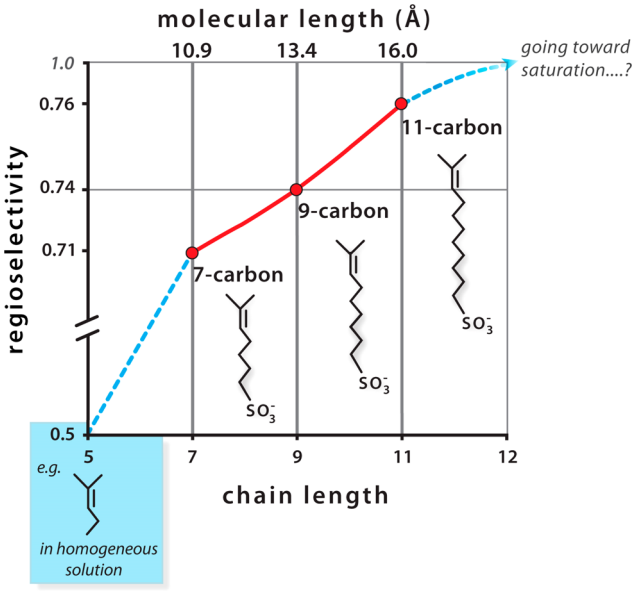

Figure 4. Effects of regioselectivity on surfactants **1**−**3** treated with airborne $^1O_2$. A saturation limit is approached in increasing the number of carbon atoms in the chain. Compounds that dissolve in common organic solvents generally show no regioselectivity, such as 2-methyl-2-pentene in the blue-colored box (ref 36). The top axis shows the molecular lengths of the surfactants.

product yield increase compared to that in H_2O, points to partial solvation of an unsymmetrical perepoxide transition state[55] in the product-determining step (Figure 5). Figure 5

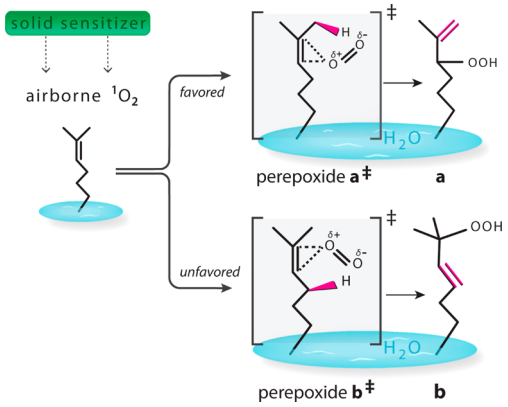

Figure 5. Proposed mechanisms for unsymmetrical and synchronous attack of $^1O_2$ on the π bond considering desolvation of the methyl groups thus favoring hydroperoxide **a** over **b**.

shows the proposed perepoxide **a**‡ that would be expected because of methyl desolvation to favor hydroperoxide **a** over **b**. In addition to perepoxides **a**‡ and **b**‡, acyclic zwitterionic species may also form as partially solvated intermediates. The 7−11-carbon length series that we have chosen also gives an approximate guide to mixed substrate and solvent quenching of $^1O_2$. For $^1O_2$ quenching, long-chain prenylsurfactants react with airborne $^1O_2$ with greater chemical quenching efficiency, while short-chain prenylsurfactants suffer from greater solvent physical quenching of $^1O_2$ because of the proximity to the liquid surface. The solubility of $^1O_2$ should be greater in the long-chain than in the short-chain surfactant so that prenyl chemical quenching ($^1O_2$ + RH → ROOH) and the appearance of hydroperoxide are facilitated for **3**, while $^1O_2$ is wasted through physical quenching for **1** ($^1O_2$ + H_2O → $^3O_2$ + H_2O). This notion is similar to facial selectivity from favored chemical over physical quenching of $^1O_2$ in oxazolidinone-functionalized enecarbamates in the literature.[56,57]

Comments about apparatus design, surfactant packing, and branching are also in order. We have utilized the delivery of $^1O_2$ in a top-down manner from a sensitizer plate to reach prenyl sites at the air−water interface. We have not conducted bottom-up studies in which a solvated sensitizer produces $^1O_2$ in solution, or aerosol studies with sunlight and solvated aromatics.[58,59] As discussed above, prenyls in long-chain surfactants extend further into the gap between the liquid surface and solid sensitizer. However, our experiments did not assess the effects of prenylsurfactants with chains shorter than that of **1**, or with chains longer than that of **3**. Thus, a wider mechanistic picture is not yet available for possible regiospecificity (saturation in Figure 4) in the hydrogen abstraction step of $^1O_2$ with prenylsurfactant. One would expect the regioselectivity and yield to become nonlinear when the carbon length is <7 and >11. Furthermore, a caveat for **1**−**3** is that they are branched, which for surfactants is a property known to cause packing that is looser than that of unbranched isomers.[60] However, **1**−**3** are branched to the same extent relative to each other, whereas the chain length is not. Our reasoning for using a prenyl group, i.e., branched trisubstituted alkene, was their higher reactivity with $^1O_2$ compared to that of a disubstituted alkene[61] for easier monitoring of the reaction in the former.

CONCLUSION

A physical−organic chemistry approach has been developed to probe $^1O_2$ at the air−water interface with the use of prenylsurfactant probes **1**−**3** and a photoreactor technique. Upon screening **1**−**3**, we find that they are effective but to different extents as interfacial traps of airborne $^1O_2$ (Figure 6).

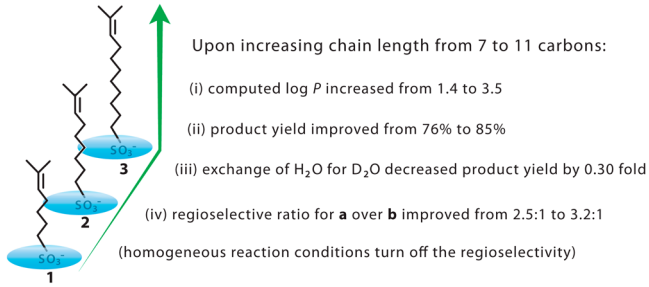

Figure 6. Mechanistic summary of "ene" reactions of airborne $^1O_2$ with surfactants **1**−**3** at the air−water interface at submicellar concentrations.

One implication of singlet oxygen at the air−water interface is its potential for broader use for selective oxidations in organic chemistry. Future studies could be undertaken (i) to examine a hydrophobic group that causes color formation upon reaction with airborne $^1O_2$ (where workup and NMR analysis and precision are not limiting factors), (ii) to compare product selectivity by theoretical methods for varying interfacial mechanisms, (iii) to examine $^1O_2$ regioselectivity based on surface tension, e.g., a perfluorinated surfactant with a surface tension lower than that of regular surfactants, (iv) to examine k_H/k_D kinetic isotope effects on H/D-substituted prenyl groups

DOI: 10.1021/acs.joc.6b01030
J. Org. Chem. 2016, 81, 6395−6401

for mechanistic insight, and (v) to expand on reactor equipment design and user accessibility to deliver ROS to air−liquid interfaces where the oxidant is delivered as a gas.

EXPERIMENTAL SECTION

Reagents, Instrumentation, and Computations. Diethyl ether, DMF, CH_2Cl_2, $CHCl_3$, ethanol, acetone, THF, pentane, hexanes, ethyl acetate, D_2O (99.8%), DMSO-d_6 (99.5%), $CDCl_3$, pyridinium chlorochromate (PCC), sodium sulfite (Na_2SO_3), sodium sulfate (Na_2SO_4), *n*-butyllithium, isopropyl triphenylphosphonium iodide, benzoic acid, aluminum(III) phthalocyanine chloride tetrasulfonic acid (AlPcS), 5-bromopentan-1-ol, 9-bromononan-1-ol, 9-bromo-2-methylnon-2-ene, Celite, silica, and porous Vycor glass were obtained from commercial sources and used as received. Water was purified using a deionization system. NMR data were recorded on a spectrometer operating at 400 MHz for ^{1}H NMR and 100.6 MHz for ^{13}C NMR. HRMS data were collected on a time-of-flight mass spectrometer. Calculations for octanol-to-water partitioning were performed with the ACD program.[39]

Synthesis of Sodium 6-Methylhept-5-Ene-1-Sulfonate (1). Yield 90 mg (16%), purity 95%.

*Step 1: Synthesis of 5-Bromo-1-pentanal (**6**).* 5-Bromo-1-pentanol **4** (0.55 g, 3.3 mmol) reacted with PCC (1.02 g, 4.90 mmol) in 50 mL of CH_2Cl_2 for 2 h at 26 °C. Fifty milliliters of Et_2O was added, and the solution was filtered with Celite to remove unreacted PCC. The residue was concentrated under vacuum, yielding 390 mg (70%) of **5** as dark-colored oil.

*Step 2: Synthesis of a Mixture of 7-Bromo-2-methylhept-2-ene (**8**) and 7-Iodo-2-methylhept-2-ene (**9**).* Isopropylphosphonium iodide (1.28 g, 3.34 mmol) in 9 mL of THF reacted with *n*-butyllithium (1.1 mL, 2.6 mmol) for 1.75 h at 0 °C. The solution was chilled to −78 °C, and then 5-bromopentanal **6** (0.35 g, 2.1 mmol) was added while the mixture was stirred for 10 min. The reaction mixture was heated to room temperature and stirred for an additional 1 h, after which the residue was extracted with pentane. It was then filtered, washed with water, and dried over Na_2SO_4. Solvent was removed by vacuum, yielding 85 mg (23%) of a mixture of **8** and **9**: ^{1}H NMR ($CDCl_3$, 400 MHz) δ 5.12 (t, J = 7.2 Hz, 1H), 3.41 (t, J = 6.8 Hz, 1H), 3.19 (t, J = 6.8 Hz, 1H), 2.00 (m, 2H), 1.84 (m, 2H), 1.64 (s, 3H), 1.60 (s, 3H), 1.43 (m, 2H); ^{13}C NMR ($CDCl_3$, 100.6 MHz) δ 132.4, 124.2, 34.3, 33.5, 32.7, 31.0, 28.7, 27.4, 27.2, 26.0, 18.0, 7.5.

Step 3: Synthesis of Sodium 6-Methylhept-5-ene-1-sulfonate (1). A Strecker reaction of **8** and **9** (∼1:1 ratio) (85 mg, 0.4 mmol) and Na_2SO_3 (0.10 g, 0.80 mmol) was conducted under a N_2 atmosphere in a refluxing DMF/water solvent (1:1) (4 mL) for 12 h. The reaction mixture was cooled to room temperature, upon which deionized H_2O (2 mL) and then ethanol (2 mL) were added. The solution was filtered and partitioned with CH_2Cl_2 (4 × 4 mL), and the CH_2Cl_2 fractions were removed. A white solid **1** was obtained after the water had evaporated: mp 227−229 °C; ^{1}H NMR (D_2O, 400 MHz) δ 5.25 (t, J = 8 Hz, 1H), 2.92 (t, J = 8 Hz, 1H), 2.05 (m, 2H), 1.74 (m, 5H), 1.64 (s, 3H), 1.60 (s, 3H), 1.47 (m, 2H); ^{13}C NMR (D_2O, 100.6 MHz) δ 133.7, 124.3, 50.9, 27.9, 26.8, 24.8, 23.6, 16.9; IR (neat) ν 2934, 2916, 2851, 1464, 1354, 1177, 1127, 1044 cm^{-1}; HRMS (TOF) m/z found $[C_8H_{15}SO_3]^-$ 191.0752, calcd $[C_8H_{15}SO_3]^-$ 191.0742.

Synthesis of Sodium 10-Methylundec-9-Ene-1-Sulfonate (3). Yield 123 mg (27%), purity 95%.

*Step 1: Synthesis of 9-Bromo-1-nonanal (**7**).* 9-Bromononan-1-ol **5** (0.57 g, 2.55 mmol) reacted with PCC (790 mg, 3.8 mmol) in 40 mL of CH_2Cl_2 for 2 h at 26 °C. Fifty milliliters of Et_2O was added, and the solution was filtered with Celite to remove unreacted PCC. The solution was washed two additional times with Et_2O. The residue was then concentrated under vacuum, yielding 467 mg (81%) of **7**.

*Step 2: Synthesis of a Mixture of 11-Bromo-2-methylundec-2-ene (**10**) and 11-Iodo-2-methylundec-2-ene (**11**).* Isopropylphosphonium iodide (1.01 g, 2.63 mmol) in 7.7 mL of THF reacted with *n*-butyllithium (0.97 mL, 2.30 mmol) for 1 h at 0 °C. The solution was chilled to −78 °C, and then 9-bromononanal **7** (0.47 g, 2.11 mmol) was added while the mixture was stirred for 30 min. The reaction mixture was heated to room temperature and stirred for an additional 1 h, after which the residue was extracted with pentane. It was then filtered, washed with water, and dried over Na_2SO_4. Solvent was removed by vacuum, yielding 168 mg (36%) of a mixture of **10** and **11**: ^{1}H NMR ($CDCl_3$, 400 MHz) δ 5.12 (t, J = 8 Hz, 1H), 3.43 (t, J = 8 Hz, 1H), 3.21 (t, J = 7.0 Hz, 1H), 1.97 (m, 2H), 1.86 (m, 2H), 1.71 (m, 3H), 1.62 (m, 3H), 1.42 (m, 2H), 1.31 (m, 8H); ^{13}C NMR ($CDCl_3$, 100.6 MHz) δ 131.2, 124.8, 34.1, 33.6, 32.8, 30.5, 29.8, 29.4, 29.2, 28.8, 28.5, 28.2, 28.0, 25.7, 17.7. 7.3.

*Step 3: Synthesis of Sodium 10-Methylundec-9-ene-1-sulfonate (**3**).* A Strecker reaction of **10** and **11** (∼1:1 ratio) (130 mg, 0.49 mmol) and Na_2SO_3 (0.12 g, 0.98 mmol) was conducted under a N_2 atmosphere in a refluxing DMF/water solvent (1:1) (8 mL) for 12 h. The reaction mixture was cooled to room temperature, upon which deionized H_2O (4 mL) and then ethanol (4 mL) were added. The solution was filtered and partitioned with CH_2Cl_2 (4 × 8 mL), and the CH_2Cl_2 fractions were removed. A white solid **3** was obtained after the water had evaporated: mp 229−232 °C; ^{1}H NMR (D_2O, 400 MHz) δ 5.26 (t, J = 8 Hz, 1H), 2.91 (t, J = 8 Hz, 2H), 2.00 (m, 2H), 1.75 (m, 2H), 1.70 (s, 3H), 1.63 (s, 3H), 1.42 (m, 2H), 1.31 (m, 8H); ^{13}C NMR (D_2O, 100.6 MHz) δ 133.1, 125.4, 51.1, 34.5, 29.0, 28.3, 28.2, 27.6, 27.2, 24.8, 23.9, 16.9; IR (neat) ν 2961, 2934, 1464, 1354, 1177, 1127, 1044 cm^{-1}; HRMS (TOF) m/z found $[C_{12}H_{23}SO_3]^-$ 247.1376, calcd $[C_{12}H_{23}SO_3]^-$ 247.1368.

Singlet Oxygen Reactor. The reactor consisted of a sensitizing glass plate made by depositing AlPcS (4 × 10^{-8} mol) onto the bottom side of a 0.50 g porous silica square (2.25 cm^2 × 1.0 mm). The sensitizing glass plate was placed on top of a quartz cuvette (1.0 cm × 1.0 cm × 0.7 cm). The sensitizer plate was placed 3.0 cm below the illumination source of (i) 669 nm light (irradiance of 383 mW cm^{-2} for 1 h; total dose of ∼1400 J/cm^2) from a diode laser with a spot size of ∼1.0 cm^2, where the cuvette receiving the 669 nm light increased in temperature by 3 °C over 1 h, or (ii) 630 nm light from Nd:YAG pumping an optical parametric oscillator (OPO) producing 5 ns pulses at ∼0.2 mJ/pulse, where singlet oxygen was directly detected by its NIR luminescence to a photomultiplier tube (PMT) by way of a 1270 nm bandpass filter (full width at half-maximum of 15 nm). τ_Δ was calculated by curve fitting with a least-squares procedure. The output of the red light from the lasers yielded incident photons in a Gaussian distribution upon the sensitizer plate. Our experiments with **1**−**3** were conducted at 1 mM, approximately $^1/_{10}$th or $^1/_3$rd of their respective CMCs, where the surfactants were gradually added and spread over the liquid. Our previous results showed that the CMC of **2** is 9.7 mM at 26 °C.[37] A digital ruler with a precision of 0.01 mm was used to measure the distance between the water surface and sensitizer plate in the cuvette. The evaporation of water in the cuvette did not cause a measurable change over the course of a 1 h photolysis experiment. Over the course of the photolysis experiment, AlPcS molecules did not become disconnected and did not relocate into the water solution. Photobleaching of the sensitizer plate occurred over ∼3 h irradiation times, after which the glass was cleaned by Soxhlet extraction and then reloaded with AlPcS. We have found with control experiments that red-light irradiation of a piece of porous Vycor bearing no AlPcS coating did not yield **2a** or **2b**. In the dark, there was no evidence of formation of hydroperoxides **a** and **b**.

Generation of Sodium 5-Hydroperoxy-6-methylhept-6-ene-1-sulfonate (1a) and Sodium (*E*)-6-Hydroperoxy-6-methylhept-4-ene-1-sulfonate (1b). Compound **1** (1 mM) was placed in the singlet oxygen reactor with 0.60 mL of D_2O for 1 h, after which the D_2O was evaporated by N_2 gas at room temperature. The ratio of **1a** and **1b** was determined by ^{1}H NMR analysis of the 11.2 and 10.8 ppm proton signals, respectively, in which benzoic acid was the internal standard: ^{1}H NMR (DMSO-d_6, 400 MHz) δ 11.28 (s, 1H), 10.82 (s, 1H), 5.54 (m, 2H), 5.50 (m, 2H), 4.87 (s, 2H), 4.84 (s, 2H) 4.12 (t, J = 8 Hz, 1H) (peaks in the aliphatic region overlap and thus are not reported).

Generation of Sodium 7-Hydroperoxy-8-methylnon-8-ene-1-sulfonate (2a) and Sodium (*E*)-8-Hydroperoxy-8-methylnon-6-ene-1-sulfonate (2b). Compound **2** (1 mM) was placed in the singlet oxygen reactor with 0.60 mL of D_2O or H_2O for 1 h, after

DOI: 10.1021/acs.joc.6b01030
J. Org. Chem. 2016, 81, 6395−6401

which the water was evaporated by N_2 gas at room temperature. The ratio of **2a** and **2b** was determined by ^{1}H NMR analysis of the 11.2 and 10.8 ppm proton signals, respectively, in which benzoic acid was the internal standard: ^{1}H NMR (DMSO-d_6, 400 MHz) δ 11.28 (s, 1H), 10.80 (s, 1H), 5.54 (m, 2H), 5.50 (m, 2H), 4.87 (s, 2H), 4.12 (t, J = 8 Hz, 1H)[37] (peaks in the aliphatic region overlap and thus are not reported).

Generation of Sodium 9-Hydroperoxy-10-methylundec-10-ene-1-sulfonate (3a) and Sodium (*E*)-10-Hydroperoxy-10-methylundec-8-ene-1-sulfonate (3b). Compound **3** (1 mM) was placed in the singlet oxygen reactor with 0.60 mL of D_2O for 1 h, after which the D_2O was evaporated by N_2 gas at room temperature. The ratio of **3a** and **3b** was determined by ^{1}H NMR analysis of the 11.2 and 10.8 ppm proton signals, respectively, in which benzoic acid was the internal standard: ^{1}H NMR (DMSO-d_6, 400 MHz) δ 11.28 (s, 1H), 10.82 (s, 1H), 5.54 (m, 2H), 5.50 (m, 2H), 4.87 (s, 2H), 4.84 (s, 2H) 4.11 (t, J = 8 Hz, 1H) (peaks in the aliphatic region overlap and thus are not reported).

■ ASSOCIATED CONTENT

Supporting Information

The Supporting Information is available free of charge on the ACS Publications website at DOI: 10.1021/acs.joc.6b01030.

HRMS, IR, and NMR spectra of surfactants **1** and **3**, NMR spectra of mixtures of **8**−**11**, and a decay trace of airborne singlet oxygen within the reactor (PDF)

■ AUTHOR INFORMATION

Corresponding Author

*E-mail: agreer@brooklyn.cuny.edu.

Notes

The authors declare no competing financial interest.

■ ACKNOWLEDGMENTS

We acknowledge support from the National Science Foundation (CHE-1464975). We also thank Milton Rosen and Leda Lee for comments.

■ REFERENCES

(1) Turro, N. J. *J. Org. Chem.* **2011**, *76*, 9863−9890.
(2) Rebek, J. *J. Org. Chem.* **2004**, *69*, 2651−2660.
(3) Durantini, A. M.; Greene, L. E.; Lincoln, R.; Martinez, S. R.; Cosa, G. *J. Am. Chem. Soc.* **2016**, *138*, 1215−1225.
(4) O'Shea, K. E.; Cardona, C. *J. Org. Chem.* **1994**, *59*, 5005−5009.
(5) Mello, R.; Martínez-Ferrer, J.; Alcalde-Aragonés, A.; Varea, T.; Acerete, R.; González-Núñez, M. E.; Asensio, G. *J. Org. Chem.* **2011**, *76*, 10129−10139.
(6) Lissi, E. A.; Encinas, M. V.; Lemp, E.; Rubio, M. A. *Chem. Rev.* **1993**, *93*, 699−723.
(7) D'Andrea, T. M.; Zhang, X.; Jochnowitz, E. B.; Lindeman, T.; Simpson, C.; David, D. E.; Curtiss, T. J.; Morris, J. R.; Ellison, G. B. *J. Phys. Chem. B* **2008**, *112*, 535−544.
(8) Kumar, J. K.; Oliver, J. S. *J. Am. Chem. Soc.* **2002**, *124*, 11307−11314.
(9) Rodgers, M. A. J.; Lee, P. C. *J. Phys. Chem.* **1984**, *88*, 3480−3484.
(10) Lee, P. C.; Rodgers, M. A. J. *J. Phys. Chem.* **1983**, *87*, 4894−4898.
(11) De Oliveira, K. T.; Miller, L. Z.; McQuade, D. T. *RSC Adv.* **2016**, *6*, 12717−12725.
(12) Gemoets, H. P. L.; Su, Y.; Shang, M.; Hessel, V.; Luque, R.; Noël, T. *Chem. Soc. Rev.* **2016**, *45*, 83−117.
(13) Ushakov, D. B.; Gilmore, K.; Kopetzki, D.; McQuade, D. T.; Seeberger, P. H. *Angew. Chem., Int. Ed.* **2014**, *53*, 557−561.
(14) Elvira, K. S.; Wootton, R. C. R.; Reis, N. M.; Mackley, M. R.; deMello, A. J. *ACS Sustainable Chem. Eng.* **2013**, *1*, 209−213.
(15) Lumley, E. K.; Dyer, C. E.; Pamme, N.; Boyle, R. W. *Org. Lett.* **2012**, *14*, 5724−5727.
(16) Yavorskyy, A.; Shvydkiv, O.; Limburg, C.; Nolan, K.; Delauré, Y. M. C.; Oelgemöller, M. *Green Chem.* **2012**, *14*, 888−892.
(17) Booker-Milburn, K. *Nat. Chem.* **2012**, *4*, 433−435.
(18) Ravelli, D.; Protti, S.; Neri, P.; Fagnoni, M.; Albini, A. A. *Green Chem.* **2011**, *13*, 1876−1884.
(19) Le Bechec, M.; Costarramone, N.; Pigot, T.; Lacombe, S. Gas-phase Photooxidation: Reactors and Materials. *Chem. Eng. Technol.* **2016**, *39*, 26−38.
(20) Tachikawa, T.; Majima, T. *J. Fluoresc.* **2007**, *17*, 727−738.
(21) Eisenberg, W. C.; Taylor, K.; Murray, R. W. *J. Phys. Chem.* **1986**, *90*, 1945−1948.
(22) Midden, W. R.; Wang, S. Y. *J. Am. Chem. Soc.* **1983**, *105*, 4129−4145.
(23) Sela, T.; Vigalok, A. *Org. Lett.* **2014**, *16*, 1964−1967.
(24) Butler, R. N.; Coyne, A. G. *Chem. Rev.* **2010**, *110*, 6302−6337.
(25) Byers, J. A.; Jamison, T. F. *J. Am. Chem. Soc.* **2009**, *131*, 6383−6385.
(26) Chanda, A.; Fokin, V. V. *Chem. Rev.* **2009**, *109*, 725−748.
(27) Pirrung, M. C.; Das Sarma, K. J.; Wang, J. *J. Org. Chem.* **2008**, *73*, 8723−8730.
(28) Breslow, R. *Acc. Chem. Res.* **1991**, *24*, 159−164.
(29) Griesbeck, A. G.; de Kiff, A. *Org. Lett.* **2013**, *15*, 2073−2075.
(30) Geer, M. F.; Walla, M. D.; Solntsev, K. M.; Strassert, C. A.; Shimizu, L. S. *J. Org. Chem.* **2013**, *78*, 5568−5578.
(31) Griesbeck, A. G.; Uhlig, J.; Sottmann, T.; Belkoura, L.; Strey, R. *Chem. - Eur. J.* **2012**, *18*, 16161−16165.
(32) Vassilikogiannakis, G.; Margaros, I.; Montagnon, T.; Stratakis, M. *Chem. - Eur. J.* **2005**, *11*, 5899−5907.
(33) Clennan, E. L.; Pace, A. *Tetrahedron* **2005**, *61*, 6665−6691.
(34) Stratakis, M.; Orfanopoulos, M. *Tetrahedron* **2000**, *56*, 1595−1615.
(35) Li, X.; Ramamurthy, V. *J. Am. Chem. Soc.* **1996**, *118*, 10666−10667.
(36) Manring, L. E.; Foote, C. S. *J. Am. Chem. Soc.* **1983**, *105*, 4710−4717.
(37) Choudhury, R.; Greer, A. *Langmuir* **2014**, *30*, 3599−3605.
(38) Malek, B.; Ghogare, A. A.; Choudhury, R.; Greer, A. *Tetrahedron Lett.* **2015**, *56*, 4505−4508.
(39) *ACD Program*; Advanced Chemistry Development Inc.: Toronto, 2015.
(40) Rosen, M. J.; Kunjappu, J. T. *Surfactants and Interfacial Phenomena*; John Wiley & Sons, Inc.: Hoboken, NJ, 2012; pp 202−215.
(41) Watkins, Z.; Taylor, J.; D'Souza, S.; Britton, J.; Nyokong, T. *J. Fluoresc.* **2015**, *25*, 1417−1429.
(42) Vilsinski, B. H.; Gerola, A. P.; Enumo, J. A.; Campanholi, K. S. S.; Pereira, P. C. S.; Braga, G.; Hioka, N.; Kimura, E.; Tessaro, A. L.; Caetano, W. *Photochem. Photobiol.* **2015**, *91*, 518−525.
(43) Scholz, M.; Dedic, R.; Breitenbach, T.; Hala, J. *Photochem. Photobiol. Sci.* **2013**, *12*, 1873−1884.
(44) Yanik, H.; Aydin, D.; Durmus, M.; Ahsen, V. *J. Photochem. Photobiol., A* **2009**, *206*, 18−26.
(45) Ostler, R. B.; Scully, A. D.; Taylor, A. G.; Gould, I. R.; Smith, T. A.; Waite, A.; Phillips, D. *Photochem. Photobiol.* **2000**, *71*, 397−404.
(46) Korytowski, W.; Bachowski, G. J.; Girotti, A. W. *Photochem. Photobiol.* **1992**, *56*, 1−8.
(47) Jensen, R. L.; Arnbjerg, J.; Ogilby, P. R. *J. Am. Chem. Soc.* **2010**, *132*, 8098−8105.
(48) Ogilby, P. R.; Foote, C. S. *J. Am. Chem. Soc.* **1982**, *104*, 2069−2070.
(49) Rodgers, M. A. J. *J. Am. Chem. Soc.* **1983**, *105*, 6201−6205.
(50) Clennan, E. L.; Chen, X. *J. Org. Chem.* **1988**, *53*, 3124−3126.
(51) Orfanopoulos, M.; Stratakis, M.; Elemes, Y. *J. Am. Chem. Soc.* **1990**, *112*, 6417−6418.
(52) Lythgoe, B.; Trippett, S. *J. Chem. Soc.* **1959**, 471−472.
(53) Davies, A. G.; Davison, I. G. E. *J. Chem. Soc., Perkin Trans. 2* **1989**, *7*, 825−30.

DOI: 10.1021/acs.joc.6b01030
J. Org. Chem. 2016, 81, 6395−6401

(54) Dang, H. S.; Davies, A. G. *J. Chem. Soc., Perkin Trans. 2* **1992**, *7*, 1095−101.
(55) Singleton, D. A.; Hang, C.; Szymanski, M. J.; Meyer, M. P.; Leach, A. G.; Kuwata, K. T.; Chen, J. S.; Greer, A.; Foote, C. S.; Houk, K. N. *J. Am. Chem. Soc.* **2003**, *125*, 1319−1328.
(56) Sivaguru, J.; Solomon, M. R.; Saito, H.; Poon, T.; Jockusch, S.; Adam, W.; Inoue, Y.; Turro, N. J. *Tetrahedron* **2006**, *62*, 6707−6717.
(57) Poon, T.; Sivaguru, J.; Franz, R.; Jockusch, S.; Martinez, C.; Washington, I.; Adam, W.; Inoue, Y.; Turro, N. J. *J. Am. Chem. Soc.* **2004**, *126*, 10498−10499.
(58) George, C.; Ammann, M.; D'Anna, B.; Donaldson, D. J.; Nizkorodov, S. A. *Chem. Rev.* **2015**, *115*, 4218−4258.
(59) Reeser, D. I.; George, C.; Donaldson, D. J. *J. Phys. Chem. A* **2009**, *113*, 8591−8595.
(60) Rosen, M. J.; Kunjappu, J. T. *Surfactants and Interfacial Phenomena*; John Wiley & Sons, Inc.: Hoboken, NJ, 2012; pp 5−6.
(61) Ghogare, A. A.; Greer, A. *Chem. Rev.* **2016**, DOI: 10.1021/acs.chemrev.5b00726.

DOI: 10.1021/acs.joc.6b01030
J. Org. Chem. 2016, 81, 6395−6401